MONTE CARLO DIFFUSION CALCULATIONS AND PLANS FOR ELECTRIC FIELD STUDIES IN HSX*

S.P. Gerhardt, J.N. Talmadge, D.T. Anderson
HSX Plasma Laboratory, U. of Wisconsin

S.A. Dettrick
Naka Fusion Research Establishment, JAERI

Abstract

A model has been developed for the asymmetric neoclassical diffusion coefficient in HSX. By fitting an analytic form of the diffusion coefficient to Monte Carlo data, the model implicitly accounts for the most important terms in the HSX magnetic field spectrum over a broad range of collisionality. It is shown how this model can be used to calculate the ambipolar electric field in the HSX Mirror mode. A short description of the instrument to measure plasma flows is described

1. Introduction

The radial electric field (E_r) in three-dimensional stellarators is determined by the ambipolarity of the asymmetric fluxes. To calculate these fluxes, it is necessary to determine the dependence of the monoenergetic diffusion coefficient on E_r and collisionality. For simple magnetic geometries, analytic models exist for the diffusion coefficient. For more realistic stellarator magnetic fields, other techniques must be used.

Models for the diffusion coefficient which include multiple-helicities have been formulated [1]. These models still rely on a simplification of the spectrum and are not necessarily valid for all collisionality regimes. This has led to the use of kinetic equation solvers to obtain diffusion coefficients.

In this paper, we take an approach to calculating the diffusion coefficient based on the work of Painter and Gardner on H-1NF [2]. In this model, the diffusion coefficient is computed using a Monte Carlo code, for many values of collisionality, E_r, particle energy, and magnetic field. We then fit this data to an analytic model for the monoenergetic diffusion coefficient, which can be integrated over moments of the distribution function. This method has the important feature that it generates an analytic expression for the diffusion coefficient which implicitly accounts for the most important terms in the magnetic spectrum

This paper is organized as follows. The magnetic geometry in the various modes of operation of HSX is discussed in Section 2. The details of the Monte Carlo calculations and the fits to the data are presented in Section 3. The paper concludes in Section 4 with a description of our instrument to measure plasma rotation in HSX.

2.HSX Magnetic Geometry

The Helically Symmetric Experiment (HSX) is the first toroidal magnetic fusion machine to posses a direction of symmetry, yet have no net plasma current [3]. This quasi-helically symmetric (QHS) magnetic field is produced by a set of modular, non-planar coils. As shown in figure #1, the magnetic spectrum is dominated by a single helical mode. In this and subsequent plots, the mode numbers are listed as [n,m], where n is the toroidal mode number for the entire machine.

Fig 1: QHS Mode Spectrum

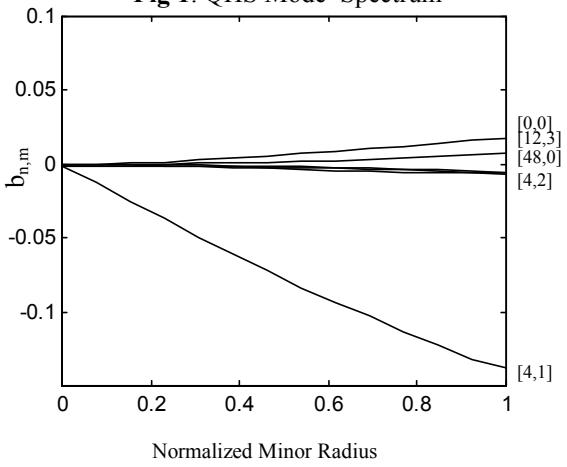

The quasi-symmetry can be broken by driving current in a set of planar auxiliary coils. One configuration of currents in these coils introduces a large mirror term to the spectrum, simulating the transport properties of a traditional three-dimensional stellarator (Figure 2). This "Mirror" mode of operation suffers from an increased number of particles on direct loss orbits, large superbanana widths, increased viscous damping, and a large increase in the diffusion coefficient.

Fig. 2: Mirror Mode Spectrum

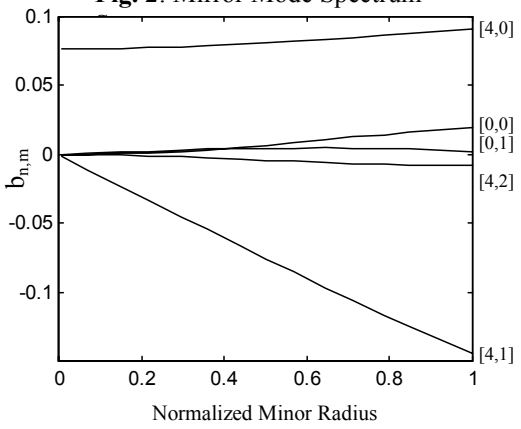

2. Monte Carlo Code and the Fitting Procedure

A Monte Carlo code was used to calculate the monoenergetic diffusion coefficient [4]. In this code, the background particle temperature and density are taken to be constant throughout the simulation volume. Typically, the background ions and electrons each have temperatures of 500 eV. The electrostatic potential is specified in the code by the form

$$\Phi(r) = \Phi_o\left(1-\left(\frac{r}{a}\right)^2\right)^2$$

To vary the electric field, simulations were run with different values of Φ_o. For each Monte Carlo data point, ensembles of 448 particles were followed; each particle was followed for at least 2 collision times. The 10 largest modes in the magnetic spectrum were used for all runs. All calculation shown in this paper were done at r/a=0.5 (r=6cm), and cutoff radii were set at ±3cm from the launch surface. Particles passing through either of these surfaces were removed from the simulation, but their statistics were kept in the calculation of D. The diffusion coefficient was calculated as in reference [5].

$$D = \frac{-4L^2}{\pi^2 t}\ln\left(\frac{1}{N}\sum_{i=1}^{N}\cos\left(\frac{\pi x_i(t)}{2L}\right)\right)$$

where L is the distance from the launch surface to the cutoff radius.

To fit the Monte Carlo data, we used expressions for both the symmetric (tokamak-like) and the asymmetric transport. To analyze the symmetric transport, a model due to Beidler was used [6]. To analyze the asymmetric component of the transport, two different analytic models were fit to Monte Carlo data. The first model, applicable to cases where E_r is large, and called the Large E_r model in this paper, is given as:

$$D_1 = \frac{4}{9\pi}(2C_1)^{\frac{3}{2}}\frac{V_d^2}{\upsilon}$$

$$D_2 = C_2 V_d^2 \frac{1}{\varepsilon_t}\sqrt{\upsilon}\frac{1}{\left(|\Omega_E|\right)^{\frac{3}{2}}}$$

$$D_3 = C_3\left(\frac{V_d}{\varepsilon_t \Omega_E}\right)^2 * \upsilon$$

$$D_{LE}^{-1} = D_1^{-1} + D_2^{-1} + D_3^{-1}$$

$$\varepsilon_t = r/R$$

$$V_d = \frac{K}{eRB}$$

Note that this model contains 3 fit parameters, C_1, C_2, & C_3, which allow the model to be fit to the Monte Carlo data. This model fails for small E_r, in that it assumes the 1/ν exists for arbitrarily small collisionality when $E_r \approx 0$.

The Extended Fit model, which allows for the diffusion coefficient to roll over for small ν, even when $E_r \approx 0$, is given as [2]:

$$D_{EX} = \frac{\sqrt{\pi}}{2}\sqrt{C_6}\varepsilon_t V_d^2 \frac{\nu}{\omega^2}$$

$$\omega^2 = C_1\tilde{\nu}^2 + C_2\left(\omega_E + \omega_B\right)^2 + C_3\omega_B^2 + C_4|\omega_B|\tilde{\nu}$$

$$\omega_B = C_5 V_d$$

$$V_d = -\frac{K}{eBr}$$

$$\tilde{\nu} = \frac{\nu}{C_6}$$

$$\omega_E = -\frac{E}{rB}$$

Note that this model has 6 fit parameters to manipulate in fitting to the Monte Carlo data.

For a given mode of machine operation (QHS or Mirror mode), a given fit model (Large E_r or Extended Fit), and a specified radius, a single set of the parameters C_i should reproduce the diffusion coefficient for a range of values of radial electric field, test particle energy, and magnetic field strength. This is to say, the parameters represent the magnetic geometry the way that ε_t and ε_h represent the geometry of a traditional stellarator.

Monte Carlo runs and their associated fits have been completed for both the mirror mode and the QHS mode of operation. Figure #3 shows the results of a scan over the parameter Φ_o for the Mirror mode. The test particles were launched with an energy of 500eV in a field of 1T, and the Large E_r model was used in the fitting. The fit parameters have the values C_1=0.117, C_2=0.0086, and C_3=0.1.

Fig 3: Mirror Mode, Scan over Φ_o Large E_r Model

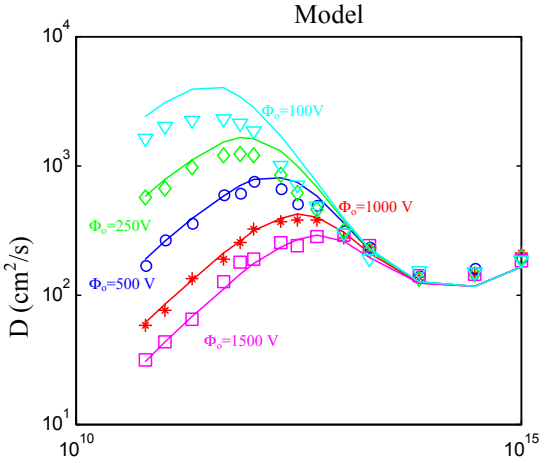

All of the curves were produced using the same set of fit parameters C_1 through C_3. Note that the poorest agreement occurs for the case with $\Phi_o = 100V < T_e/e$.

Figures #4 and #5 show that the model can also reproduce the results of Monte Carlo scans over test particle energy and magnetic field on axis. The fit parameters are identical to those used in producing Figure #3.

Fig 4: Mirror Mode Scan over Test Particle Energy, Large E_r Model

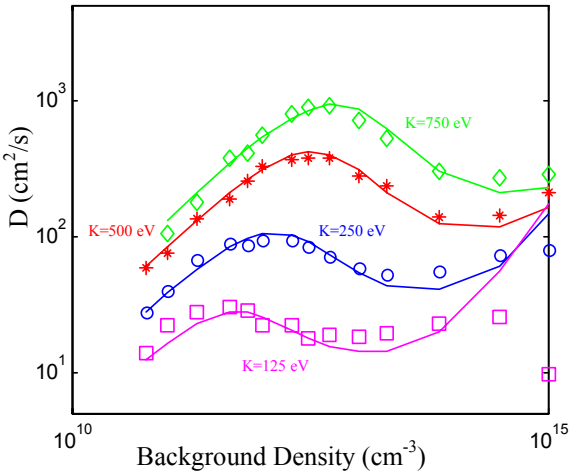

Fig 5: Mirror Mode Scan over B_o, Large E_r Model

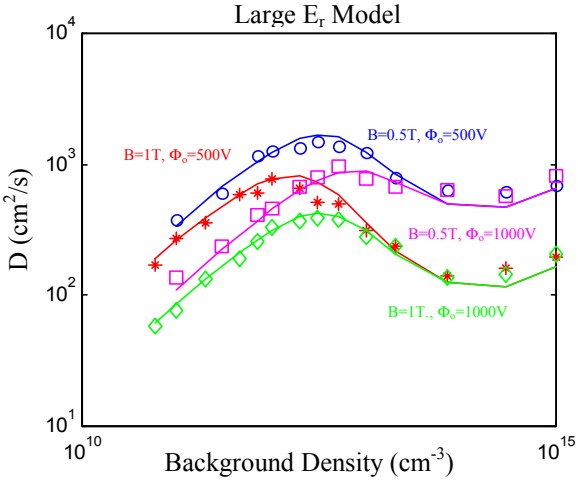

The scan over B_o demonstrates interesting scaling. In the high density regime, where the symmetric transport dominates, the diffusion coefficient is independent of E_r and proportional to B^{-2}. In the extreme low collisionality limit (the "ν" regime), the diffusion coefficient is independent of B and scales as E_r^{-2}.

As an example of the fits attainable using the Extended Fit model, a scan over the parameter Φ_o at r/a=0.5 is shown in Figure #6. This data is similar to that shown in Figure #3, except that Monte Carlo data for $E_r \approx 0$ is shown, and the fits are done with the extended fit model. The parameters used are C_1=196, C_2=6.8, C_3=772, C_4=1948, C_5=-.23, and C_6=.502.

Fig 6: Mirror Mode, Scan over Φ_o Large E_r Model

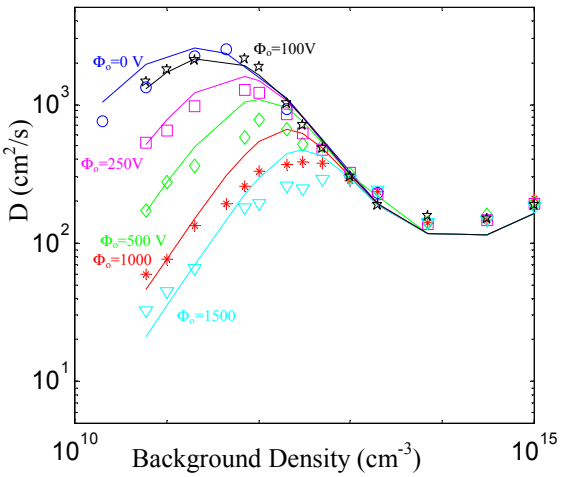

Note that this model is able to reproduce the results of calculation near E_r=0, at the expense of some accuracy at larger E_r.

Equivalent calculations have been performed for the QHS mode of operation. Figure #7 shows the result of a scan over Φ_o for fixed particle energy of K=500eV; the fits are performed using the Large E_r model.

Fig 7: QHS Mode scan over Φ_o, Large E_r Model

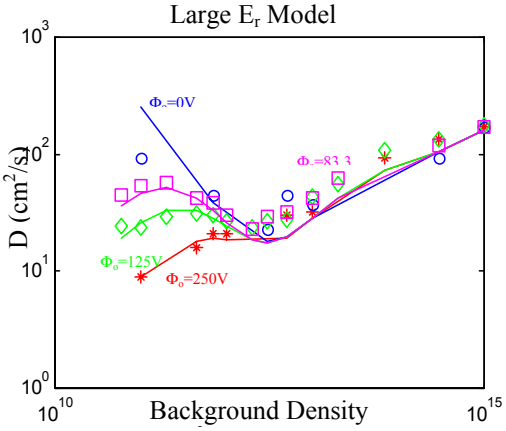

Note that in the QHS mode, the diffusion coefficient is about 2 orders of magnitude smaller than in the Mirror mode. The QHS mode has a small 1/ν regime, due

to the small residual symmetry breaking terms. As the data shows, this 1/ν regime is effectively killed by even a small value of E_r.

5. Ambipolarity Calculations

One application of these calculations is the calculation of the ambipolar electric field in the HSX Mirror mode. This electric field is determined by forcing the ion and electron fluxes to be equal to each other on each flux surface [7]:

$$\sum_{s=i,e} \Gamma_s\left(r, E_r\right) = 0$$

In this expression, the fluxes are determined by an integral over the distribution function as:

$$\Gamma_s = \frac{-n_s}{\sqrt{\pi}} \int D_s(x, r, \frac{d\Phi}{dr}) e^{-x} \sqrt{x} G(x) dx$$

$$G(x) = \frac{1}{n_s}\frac{dn_s}{dr} + \frac{1}{T_s}\frac{d\Phi}{dr} + \frac{1}{T_s}\frac{dT}{dr}\left(x - \frac{3}{2}\right)$$

For the ambipolarity calculations presented here, the following profiles are assumed:

$$n_s(r) = 5x10^{12}\left(1 - \left(\frac{r}{a}\right)^6\right) = n_e(r)$$

$$T_i(r) = 200\left(1 - \left(\frac{r}{a}\right)^6\right)$$

$$T_e(r) = 500\left(1 - \left(\frac{r}{a}\right)^5\right)$$

In these formulas, densities are measured in cm^{-3} and temperatures in eV. Note that these profiles are not necessarily consistent with each other nor with the E_r value that is calculate from them. Using these assumed profiles, Γ_e and Γ_i are plotted as a function of E_r. The intersection of the two curves gives the value of E_r which satisfies the ambipolarity constraint. Figure #8 shows the results of such an ambipolarity calculation using the Large E_r model. The calculation is done at r/a=0.5.

Figure #8 :Mirror Mode Ambipolarity Calculation using the Large E_r model.

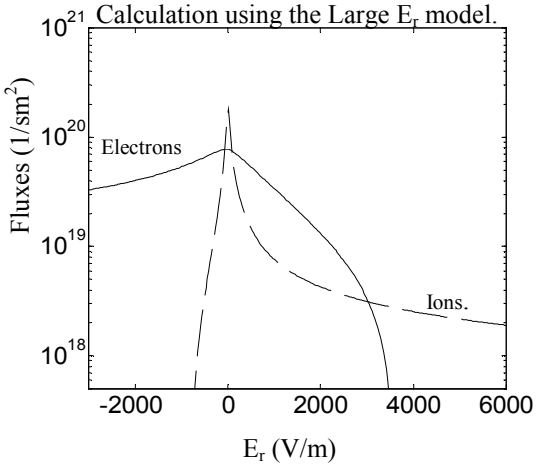

This calculation shows three possible roots to the ambipolarity constraint, at E_r=3020 V/m, 85 V/m, and –70 V/m.

The same calculation can be done using the Extended Fit model for the diffusion coefficient, leading to different results as shown in Figure #9.

Figure #9 :Mirror Mode Ambipolarity Calculation using the Extended Fit model.

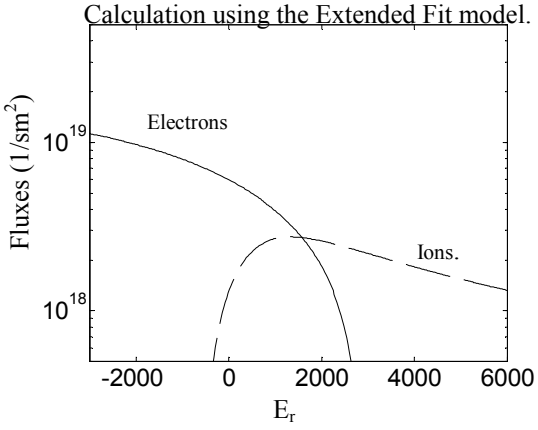

Note that the large peaks in the fluxes near E_r=0 are not seen in this model, but that both models predict roughly the same fluxes for large values of E_r. As can be seen from the plot, this model predicts only one root at E_r = 1500V/m. This value of E_r corresponds to Φ_o=120V. As was shown above, for these small fields, the Extended Fit model fits the Monte Carlo

data more accurately than the Large E_r model. Hence, the second ambipolarity calculation is more accurate within the bounds of this simple calculation. It should also be mentioned that this method of calculating E_r is not thought to be accurate for the QHS mode of operation, where it was shown earlier that the stellarator transport is only a small addition to the axisymmetric part. Hence, the fluxes are not shown for the QHS case.

Further work on this subject will extend the fits across the full minor radius of HSX. Once the fit parameters for the two models have been determined as a function of minor radius, the asymmetric diffusion coefficient will be inserted into the 1D transport modeling code ASTRA. This will allow self-consistent density, temperature, and electric field profiles to be computed and compared to experimental data.

6. Experimental Plans

We plan to measure the plasma flow in HSX via Doppler spectroscopy using a 1-meter spectrometer. The detector is a 1024x256 element back-illuminated CCD detector with 26μm by 26μm pixels. The grating has 3600 grooves/mm, providing a dispersion of .006 nm/pixel in 1st order. Assuming that .1 pixel is resolvable, this leads to a flow resolution of ≈800 m/s. The instrument is operated under LabVIEW control and integrated into the HSX data system. Light is coupled to the instrument via a fiber bundle which is split so as to have two input channels

Initially, plasma light will be collected from two poloidal chords on the miniflange array, as shown in Figure #10.

Fig. #10: Viewing Chords for Rotation Measurement

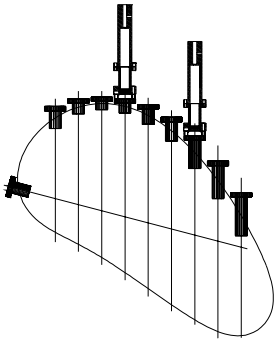

This arrangement allows for the calculation of the chord-averaged difference in the flow velocity between the two chords. This difference in flow velocity can then be compared to theoretical models. Plans are underway to extend the spectrometer views to include full poloidal flow profile information and toroidal flow measurements. Future plans include breaking the input fiber into more bundles to increase the total number of channels.

References

[1] K.C. Shaing and S.A. Hokin, 1983 Phys, Fluids **26** 2136
[2] S.L. Painter and H.J. Gardner, 1993 Nuclear Fusion **33** 1107
[3] F.S.B. Anderson, A.F Almagri, D.T. Anderson, P.G. Matthews, J.N. Talmadge and J.L. Shohet, 1995 Trans. Of Fusion Technology **27** 273.
[4] C. Beidler, Private Communication
[5] C.D. Beidler, Ph.D. thesis, U. of Wisconsin-Madison.
[6] C. D. Beidler and W.N.G Hitchon, 1994 Plasma Phys. Control. Fusion **36** 317
[7] H.E. Mynick and W.N.G. Hitchon, 1983 Nuclear Fusion **23** 1053

*This work is sponsored by the U.S. Department of Energy